Molecular Cancer Therapeutics

Tyrosine Threonine Kinase Inhibition Eliminates Lung Cancers by Augmenting Apoptosis and Polyploidy

Lin Zheng[1], Zibo Chen[1,2], Masanori Kawakami[1,2], Yulong Chen[1], Jason Roszik[3,4], Lisa Maria Mustachio[1], Jonathan M. Kurie[1], Pamela Villalobos[5], Wei Lu[5], Carmen Behrens[5], Barbara Mino[5], Luisa M. Solis[5], Jennifer Silvester[6], Kelsie L. Thu[6], David W Cescon[6], Jaime Rodriguez-Canales[5], Ignacio I. Wistuba[5], Tak W. Mak[6], Xi Liu[1,2], and Ethan Dmitrovsky[1,2,7]

Abstract

The spindle assembly checkpoint maintains genomic integrity. A key component is tyrosine threonine kinase (TTK, also known as Mps1). TTK antagonism is hypothesized to cause genomic instability and cell death. Interrogating The Cancer Genome Atlas revealed high TTK expression in lung adenocarcinomas and squamous cell cancers versus the normal lung ($P < 0.001$). This correlated with an unfavorable prognosis in examined lung adenocarcinoma cases ($P = 0.007$). TTK expression profiles in lung tumors were independently assessed by RNA *in situ* hybridization. CFI-402257 is a highly selective TTK inhibitor. Its potent antineoplastic effects are reported here against a panel of well-characterized murine and human lung cancer cell lines. Significant antitumorigenic activity followed independent treatments of athymic mice bearing human lung cancer xenografts (6.5 mg/kg, $P < 0.05$; 8.5 mg/kg, $P < 0.01$) and immunocompetent mice with syngeneic lung cancers ($P < 0.001$). CFI-402257 antineoplastic mechanisms were explored. CFI-402257 triggered aneuploidy and apoptotic death of lung cancer cells without changing centrosome number. Reverse phase protein arrays (RPPA) of vehicle versus CFI-402257–treated lung cancers were examined using more than 300 critical growth-regulatory proteins. RPPA bioinformatic analyses discovered CFI-402257 enhanced MAPK signaling, implicating MAPK antagonism in augmenting TTK inhibitory effects. This was independently confirmed using genetic and pharmacologic repression of MAPK that promoted CFI-402257 anticancer actions. TTK antagonism exerted marked antineoplastic effects against lung cancers and MAPK inhibition cooperated. Future work should determine whether CFI-402257 treatment alone or with a MAPK inhibitor is active in the lung cancer clinic.

Introduction

Altered cell-cycle progression is a hallmark of cancer (1, 2). Fidelity of the cell cycle is monitored by checkpoints to ensure that essential steps are properly completed before initiation of subsequent phases (3). The spindle assembly checkpoint (SAC) is a conserved pathway in eukaryotes that arrests the cell cycle in mitosis until all chromosomes form stable bipolar attachments to the mitotic spindle (4). Defects in SAC function result in chromosome missegregation by allowing mitotic exit in the presence of unattached kinetochores (5–7). It is previously reported that SAC inactivation generates lethal genomic instability in cancer cells (8–10).

Tyrosine threonine kinase (TTK, also called Msp1), is a key component of SAC; it was identified as a surveillance mechanism to ensure mitotic fidelity and genome stability (11). Cancers such as lung cancers are highly proliferative, especially those that are most lethal, and thereby have high levels of expression of cell-cycle–expressed genes, including TTK (12). TTK inhibition causes premature exit from mitosis with unattached chromosomes. This confers deleterious chromosome missegregation, aneuploidy, and ultimately cell death (5, 8–10, 13). Reduced TTK activity substantially decreases cell viability (10, 14). Enhanced TTK mRNA expression was frequently found in breast cancers, including triple-negative breast cancers (14, 15). Intriguingly, TTK was highlighted as an attractive antineoplastic target through comprehensive analysis that combined RNAi screening with gene expression profiles of human breast cancers (14). TTK mRNA levels were elevated in hepatocellular carcinoma, pancreatic cancer, gastric cancer, and other cancers (16–18).

[1]Department of Thoracic/Head and Neck Medical Oncology, The University of Texas MD Anderson Cancer Center, Houston, Texas. [2]Frederick National Laboratory for Cancer Research, Frederick, Maryland. [3]Department of Melanoma Medical Oncology, The University of Texas MD Anderson Cancer Center, Houston, Texas. [4]Department of Genomic Medicine, The University of Texas MD Anderson Cancer Center, Houston, Texas. [5]Department of Translational Molecular Pathology, The University of Texas MD Anderson Cancer Center, Houston, Texas. [6]The Campbell Family Institute for Breast Cancer Research at Princess Margaret Cancer Centre, University Health Network, Toronto, Ontario, Canada. [7]Department of Cancer Biology, The University of Texas MD Anderson Cancer Center, Houston, Texas.

Note: Supplementary data for this article are available at Molecular Cancer Therapeutics Online (http://mct.aacrjournals.org/).

L. Zheng and Z. Chen contributed equally to this article.

Corresponding Author: Ethan Dmitrovsky, Leidos Biomedical Research, P.O. Box B, Frederick, MD 21702. Phone: 301-846-1154; Fax: 301-228-4914; E-mail: ethan.dmitrovsky@nih.gov

Mol Cancer Ther 2019;18:1775–86

doi: 10.1158/1535-7163.MCT-18-0864

This study confirmed and extended prior work by reporting TTK mRNA expression [as assessed using The Cancer Genome Atlas (TCGA)] was significantly higher in human lung adenocarcinomas and squamous cell carcinomas (SCC), as compared with normal lung tissues. These expression findings were independently assessed by RNA *in situ* hybridization (RNA-ISH) of tissue microarrays (TMA) of human lung cancers versus normal lung tissue. The findings revealed a link existed between TTK expression and lung cancer biology.

To explore directly this relationship further, antineoplastic activity of the TTK inhibitor, CFI-402257, was explored against lung cancers. This selective TTK inhibitor (Supplementary Fig. S1) exerts potent TTK antagonism and anticancer effects *in vitro* and *in vivo* (14, 19). It is undergoing testing as part of a phase I clinical trial for treatment of advanced solid tumors (ClinicalTrials.gov ID: NCT02792465). One limitation of prior work was that antineoplastic activity was not previously studied in lung cancer, the leading cause of cancer-related death for men and women (20).

This study addressed this knowledge gap by systematically examining CFI-402257 antineoplastic activity in murine and human lung cancer cell lines, as well as in syngeneic and athymic murine lung cancer models. Engaged TTK inhibitor mechanisms were elucidated. Prominent increases in polyploidy were observed in these cancer cells after CFI-402257 treatment. This was associated with increased apoptotic cancer cell death. Translational relevance of this work was confirmed by analysis of TTK expression profiles in lung cancers using TCGA and by RNA-ISH analysis of lung cancer TMAs. TTK expression in lung cancers was compared with that of proliferation markers.

Aneuploidy is a hallmark of cancer (21). It is a frequent feature of human cancers and is associated with a poor prognosis (21, 22). Aneuploidy can have detrimental effects on cellular homeostasis and survival by promoting apoptosis (22).

This study found that the TTK inhibitor, CFI-402257, elicits marked anticancer effects in lung cancer by augmenting polyploidy and apoptosis. Reverse phase protein array (RPPA) is a useful tool to elucidate whether other pathways are engaged by TTK antagonism. Candidate pharmacologic targets that could cooperate with TTK inhibition were uncovered and included augmented MAPK pathway signaling. Antagonism of MAPK pathway was shown to increase CFI-402257 antineoplastic activity. Taken together, the findings presented here indicate that TTK antagonism holds promise for combating lung cancers, especially in concert with a MAPK inhibitor.

Materials and Methods

Data sets

Gene expression profiles and clinical data for the studied lung cancer cases along with histologically normal lung tissues were obtained from TCGA, as described previously (23, 24). We used in these analyses rnaseqv2 Level 3 RSEM data downloaded from this link: http://gdac.broadinstitute.org/runs/stddata__2016_01_28/.

Chemicals and cell culture

CFI-402257 was obtained from Dr. Tak Mak (Princess Margaret Cancer Centre, Toronto, Canada). SCH772984 was purchased (Selleck Chemicals). Murine lung cancer cell lines ED1, 393P, and LKR13 were derived from lung cancers of wild-type cyclin E, $Kras^{LA1/+p53\ R172\triangle G}$ and $Kras^{LA1/+}$ transgenic mice, respectively, and were authenticated as described previously (25–29). Human lung cancer cell lines A549, H1299, and H226 were authenticated by and purchased from ATCC. These cells were cultured, as described before (27).

ISH

TTK ISH profiles were obtained from 259 formalin-fixed, paraffin embedded (FFPE) resected non–small cell lung carcinomas (NSCLC) with each case placed in a TMA. All cases underwent surgical resection at The University of Texas MD Anderson Cancer Center (Houston, TX). Written informed consent was obtained from all patients under a protocol approved by the institutional review board. Patient study was conducted in accordance with Declaration of Helsinki, International Ethical Guidelines for Biomedical Research Involving Human Subjects (CIOMS), Belmont Report, and U.S. Common Rule.

TTK ISH was performed using an automated RNAscope assay and the Leica Bond RX Autostainer (Leica Microsystems) to visualize individual RNA molecules in cells as single signals in FFPE specimens. The ISH was performed using the BOND RX system. In brief, 5-μm thick tissue sections were deparaffinized and rehydrated following the Leica Bond protocol; antigen retrieval was with ER2 (BOND Epitope Retrieval Solution 2) at 95°C for 15 minutes and ACD Protease treatment at 40°C for 15 minutes; and RNA-specific probes were hybridized to target RNA for 120 minutes at 42°C. Signals were amplified in multiple steps, which were followed by hybridization to horseradish peroxidase–labeled probes. Detection was with the 3,3-diaminobenzidine chromogenic substrate. Cells were counterstained with hematoxylin. These RNAscope probes were examined: TTK (target probe; Hs-TTK, 445138, Advanced Cell Diagnostic), housekeeping gene PPIB (positive control; Hs-PPIB, 313908, Advanced Cell Diagnostic), and bacterial gene DapB (negative control; 312038, Advanced Cell Diagnostic). Positive and negative controls were used.

RNA-ISH slides were digitally scanned using the Aperio ScanScope AT2 (Leica Microsystems) with 40 × objective magnification. TTK RNA expression was evaluated using an Aperio Image Toolbox and the RNA ISHv2 algorithm. Signals were quantified and an H-score was obtained, as follows: cells expressing the target probe were scored as category levels of 0 (no staining), 1+ (1–5 dots/cell), 2+ (6–20 dots/cell), and 3+ (21 or more dots/cell). The extent of expression was reported as the percentage of cells within each scored group. The final H-score was obtained by multiplying the respective category levels and values (range, 0–300).

siRNA transfections

Human and murine TTK-targeting siRNAs were purchased (GE Healthcare). Target sequences were: ON-TARGETplus nontargeting control pool (D-001810-10) that served as control siRNA, human TTK siRNA1 (J-004105-10): GCAAUACCUUGGAUGAUUA; human TTK siRNA2 (J-004105-12): GAUAGUUGAUGGAAUGCUA; murine Ttk siRNA 1(J-047162-07): UCAGUUAACGGAAGAAUUU; and the murine Ttk siRNA2 (J-047162-08): GAUGGAAUGCUAAAGCUAA. Cells were transfected with siRNA at a final concentration of 100 nmol/L using DharmaFECT Duo Transfection Reagent (GE Healthcare). Five days (A549, H1299, and H226) or 4 days (ED1, 393P, and

LKR13) after transfection, cell viabilities were measured using WST-1 Reagent (Takara), according to the manufacturer's recommendations. Nontargeting control siRNAs were screened by genome-wide microarray analyses to establish minimal off-target effects. The negligible effects of transfected control siRNAs on cell viability were used to normalize the observed experimental siRNA-mediated effects.

Proliferation assay

Cell proliferation was assessed by the sulforhodamine B colorimetric assay using previously optimized methods (30).

Apoptosis analysis

Cells treated with vehicle, DMSO, or CFI-402257 for 3 days were harvested and stained with Annexin V/propidium iodide, and analyzed following established methods (24).

Multipolar anaphase assays

Multipolar anaphase assays were conducted following established methods (31). For centrosome and mitotic analyses cells were fixed and stained with the anti-α-tubulin–specific antibody and with DAPI before mounting with Pro-Long Gold antifade reagent. Stained cells were scored for multipolar anaphase cells using an Eclipse TE 2000-E microscope (Nikon). Primary antibodies were α-tubulin (NB600-506; Novus Biologicals; 1:1,500) and γ-tubulin (T5326; Sigma Aldrich; 1:1,000). Secondary antibodies were Texas red anti-murine IgG (H + L) (TI-2000; Vector Laboratories; 1:500), Alexa Fluor 594 anti-rat IgG (A21209; Invitrogen; 1:1,000), and fluorescein anti-murine IgG (FI-2000; Vector Laboratories; 1:100). Hoechst 33342 (62249; Thermo Fisher Scientific; 1:10,000) stained for DNA. Pro-Long Gold anti-fade Reagent (P36934; Invitrogen) preserved immunofluorescence.

DNA polyploidy analysis

DNA polyploidy analyses were conducted following optimized methods (14). After 48 hours of treatment with vehicle (DMSO), CFI-402257, or other drug treatments, cells were harvested and fixed in 70% ethanol at −20°C for at least 4 hours. Cells were then stained with propidium iodide (PI)/RNase Staining Solution (Cell Signaling Technology) and analyzed by flow cytometer (BD Biosciences). DNA polyploidy was scored when observed peaks were beyond the diploid to tetraploid range.

In vivo experiments

All murine tumorigenicity studies were performed after the proposed studies were reviewed and approved by the MD Anderson Cancer Center Institutional Animal Care and Use Committee. 393P murine lung cancer or H1299 human lung cancer cells were injected subcutaneously into 6- to 8-week-old immunocompetent 129S2/SVPasCrl mice or immunodeficient athymic mice, respectively (Charles River Laboratories). When the tumors reached a mean size of 100 mm^3, mice were randomized into vehicle or CFI-402257 treatment groups. Mice received vehicle (90% PEG-400) or CFI-402257 treatments at the indicated dosages for 21 days by oral gavage ($n = 15$ mice per group). Tumor volume (V) was calculated as $V = (\text{length} \times \text{width}^2)/2$. The individual relative tumor volume (RTV) was calculated according to the formula: $RTV = V_n/V_0$, where V_n was tumor volume on day n and V_0 was tumor volume on the first day of treatment.

RPPA

RPPA analyses were performed using cell lysates from syngeneic 393P lung cancer cell line–derived xenografts from mice treated with vehicle or CFI-402257 for 5 days ($n = 5$ mice per group). Cell lysates were arrayed on nitrocellulose-coated slides and probed individually with 304 antibodies that respectively recognize specific growth-regulatory proteins, as described previously (24).

Immunoblot analyses

After treatment, cells were lysed using ice-cold RIPA buffer with protease inhibitors (Selleck Chemicals) before immunoblotting was done as in prior work (24).

Statistical analysis

Dose-response data were analyzed with nonlinear regression using GraphPad Prism. RPPA and gene expression data from RNA-sequencing of TCGA were obtained from public TCGA data repositories. Kaplan–Meier survival analyses were performed using the "survival" R package. Spearman rank correlation coefficients were determined using the R software. When comparing two groups, two-tailed Student t tests were used. Differences and correlations were considered significant when $P < 0.05$. Combination treatments were assessed, as described previously (32).

Results

TTK expression profiles in human lung cancers

TTK mRNA expression profiles within human lung cancers were analyzed using TCGA database. Findings revealed that TTK levels were statistically significantly higher in both adenocarcinomas ($P < 0.001$) and SCCs ($P < 0.001$) as compared with those in normal lung tissues (Fig. 1A). The elevated levels of TTK expression in lung adenocarcinomas were associated with an unfavorable survival ($P < 0.01$), as displayed in Fig. 1B. TTK mRNA expression levels varied within lung cancer TMAs, as in the representative photomicrographs of Fig. 1C. Higher TTK RNA-ISH expression had a trend to reduced survival in lung adenocarcinomas, as shown in Fig. 1D. In NSCLC TMAs, there was a statistically significant positive correlation (Spearman $\rho = 0.259$; $P = 0.000188$) between TTK mRNA expression and Ki-67 expression, as in Fig. 1E. TCGA NSCLC database confirmed that TTK mRNA positively correlated with Ki-67 expression (Spearman $\rho = 0.799$ for adenocarcinomas, Spearman $\rho = 0.511$ for SCCs) and PCNA expression (Spearman $\rho = 0.737$ for adenocarcinomas, Spearman $\rho = 0.0.481$ for SCCs). All of these correlations are highly statistically significant, as displayed in Fig. 1E. Notably, TTK mRNA ISH expression was higher in former and current smokers than in nonsmokers with lung cancers (Supplementary Fig. S2A). These clinical associations provided a rationale for studying the antineoplastic effects of antagonizing TTK activity in lung cancer cells, as was next examined.

Antiproliferative effects of CFI-402257

The TTK inhibitor used (CFI-402257) was designed on the basis of a scaffold hopping strategy and was optimized as a selective agent with favorable oral bioavailability (14, 19). To determine the antineoplastic activity of CFI-402257 in lung cancer, dose-dependent proliferation responses were explored using different drug concentrations in genetically defined

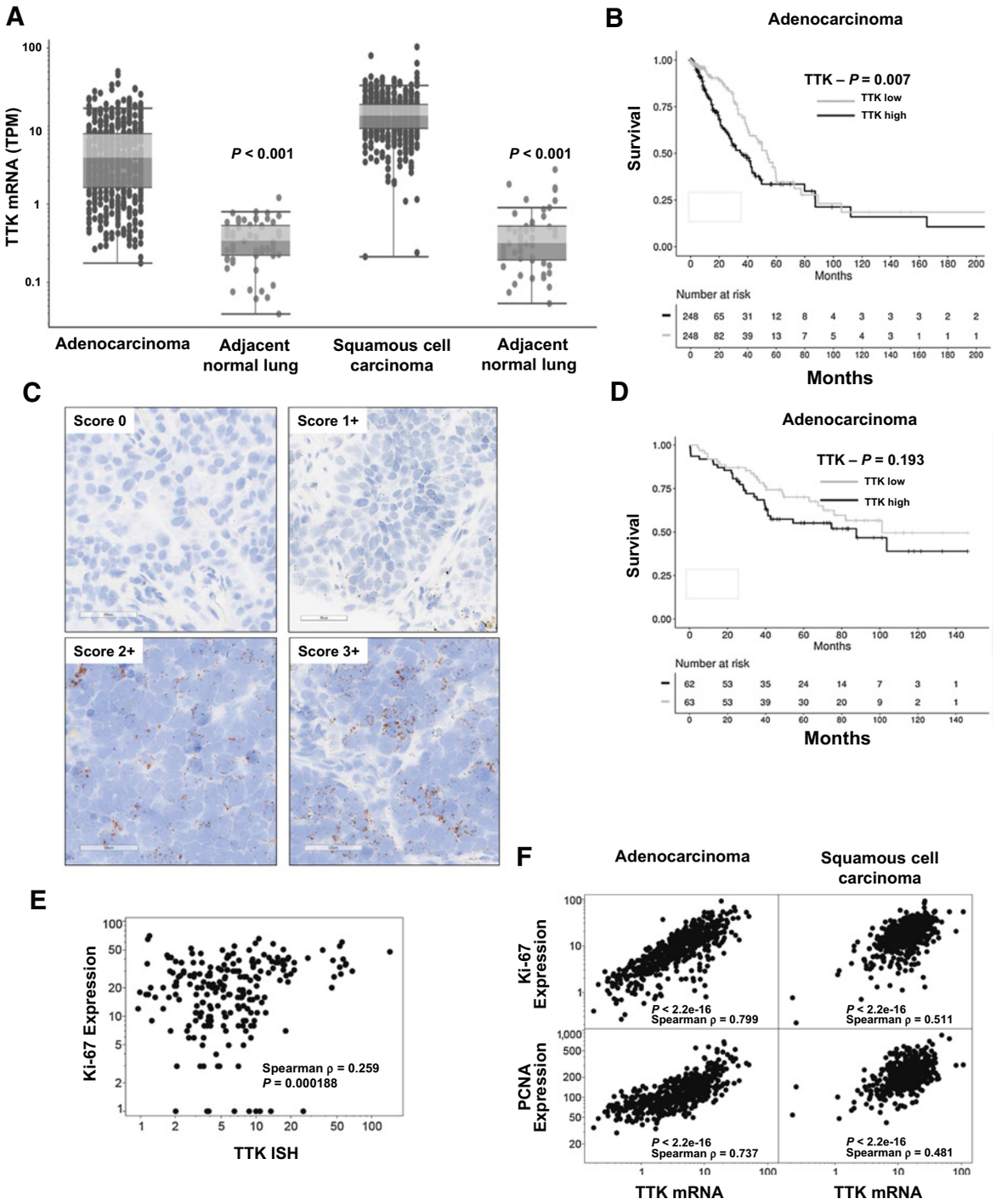

Figure 1.

TTK expression profiles in human lung cancers. **A,** Comparison of TTK mRNA expression between normal (N) and malignant (T) lung, including adenocarcinomas and SCCs within TCGA databases ($n = 517$ for malignant, 59 for normal in adenocarcinoma; $n = 501$ for malignant, 51 for normal in SCC). **B,** Comparison of survival between TTK-high versus -low expressing cases in adenocarcinomas within TCGA databases (the number of cases is displayed). **C,** Microphotographs showing human NSCLCs (a representative score 0 case is adenocarcinoma and the other displayed cases are SCCs) with different levels of TTK RNA-ISH expression in malignant cells: 0 (no staining), 1+ (1–5 dots/cell), 2+ (6–20 dots/cell), and 3+ (21 or more dots/cell). Scale bars are shown. **D,** Kaplan–Meier survival comparisons of TTK-high versus -low expression levels (using the median H-score as a cut-off point) in adenocarcinomas using NSCLC microarrays (the number of studied cases is shown). **E,** Association between TTK RNA-ISH expression and Ki67 IHC in NSCLC TMA. **F,** Associations between TTK mRNA and Ki-67 expression as well as TTK mRNA and PNCA expression profiles in adenocarcinomas and SCCs present within TCGA databases.

murine lung cancer cell lines (ED1, 393P, and LKR13) and treatments over 3 days with comparisons made with vehicle controls. CFI-402257 exerted potent growth-inhibitory responses in the studied murine lung cancer cell lines that were derived from transgenic mice whose tumors were driven by *KRAS* and/or p53 expression. Following 3 days treatment of cells with CFI-402257 (10 nmol/L dosage), marked growth inhibition (relative to controls) was observed in each of these murine lung cancer cell lines, as shown in Fig. 2A–C. The consequences of CFI-402257 treatments were examined further in the following human lung cancer cells lines: A549, H1299, and H226. As displayed in Fig. 2D–F, human lung cancer cells

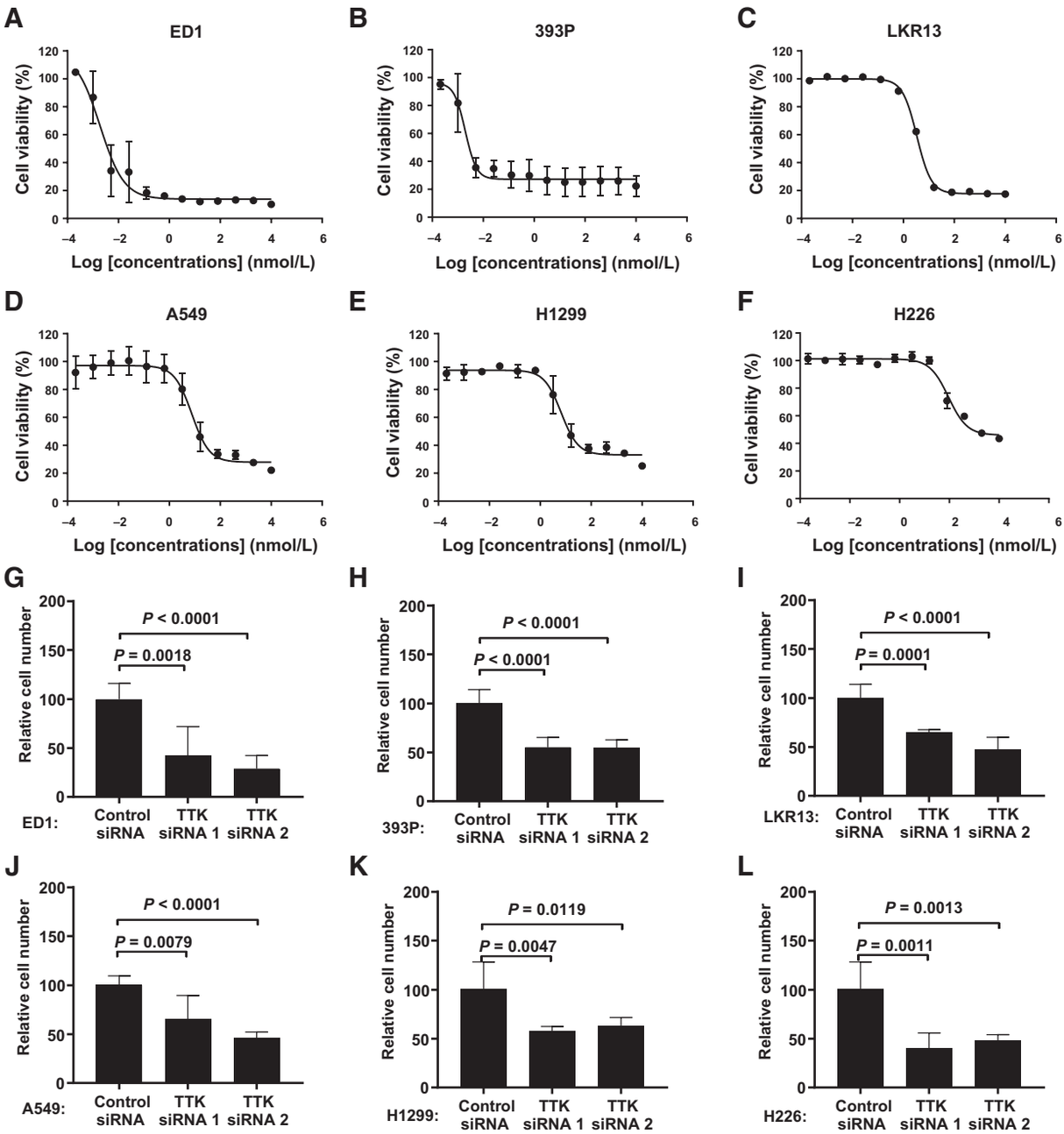

Figure 2.

A–F, Antiproliferative effects of CFI-402257 treatment in the indicated murine and human lung cancer cell lines. Dose-response curves are displayed for the indicated murine (ED1, 393P, and LKR13) and human (A549, H1299, and H226) lung cancer cell lines after CFI-402257 treatment for 72 hours. The indicated murine (**G–I**) and human (**J–L**) lung cancer cells were individually transfected with one of two different TTK-targeting siRNAs (at a final concentration of 100 nmol/L). Cell viabilities were measured 5 days (for human cells) or 4 days (for murine cells) after transfection. The *P* values are two-tailed Student *t* tests.

also responded markedly to CFI-402257 treatments (IC_{50} for A549, 7.6 nmol/L; for H1299, 6.6 nmol/L; and for H226, 92.1 nmol/L) even in cells known to express the *KRAS* oncoprotein and/or the mutant p53 protein, as reviewed (33). Human adenocarcinoma cell lines are frequently sensitive to CFI-402257 treatment and are shown in Supplementary Fig. S2B.

To confirm independently that TTK was an anticancer target, a genetic strategy was used to reduce TTK expression in murine and human lung cancer cells using independent siRNA-based transfections with two different TTK-targeting siRNAs versus control siRNAs. Efficient knockdown of TTK expression was confirmed by immunoblot analysis (Supplementary Fig. S3). Reduction of TTK expression by use of siRNAs significantly inhibited the growth of both murine (Fig. 2G–I) and human (Fig. 2J–L) lung cancer cells.

Whether CFI-402257 treatment of lung cancer cell lines that harbor wild-type (ED1, H1299, and H226) or mutant (393P, LKR13, and A549) *KRAS* species or those that express wild-type (ED1, LKR13, A549), mutant (393P and H226), or deficient (H1299) *p53* species had different response profiles was examined. The data presented in Fig. 2 confirmed that *KRAS* or p53 mutations alone or cells with dual *KRAS*/*p53* mutations, respectively, did not alter the response of these lung cancer cell lines to CFI-402257 treatments.

CFI-402257 promotes apoptosis and polyploidy

Centrosome deregulation is a frequent feature of human cancers (34). TTK-dependent SAC activity plays an important role in protecting against the deleterious consequences of supernumerary centrosomes by enabling bipolar spindle assembly and preventing multipolar cell division (35, 36). There are reports that question whether TTK inhibitors affect centrosome duplication or multipolar cell division (37–40). However, appreciable differences were not detected in centrosome numbers or in the percentages of multipolar anaphase lung cancer cells between vehicle- and CFI-402257–treated cellular populations, as depicted in Fig. 3A and B.

Inhibition of TTK activity is reported to promote chromosome missegregation, polyploidy, and cell death (5, 9, 10, 41–43). Given this, it was determined whether CFI-402257 treatment augmented polyploidy. As displayed in Fig. 3C, CFI-402257 treatment (at dosages of 40, 200, or 1,000 nmol/L) produced a statistically significant increase in the proportion of lung cancer cells that exhibited an aneuploid DNA content. Not surprisingly, CFI-402257 induction of polyploidy was accompanied by a statistically significant promotion of apoptotic cells after this treatment, as shown in Fig. 3D.

CFI-402257 treatment and *in vivo* tumorigenicity

In vivo CFI-402257 antineoplastic effects in lung cancers were examined using two models displayed in Fig. 4. The first was the 393P murine lung cancer syngeneic model and the second was the H1299 human lung cancer xenograft model in athymic mice. 393P and H1299 lung cancer cells were independently subcutaneously injected into immunocompetent syngeneic mice and immunodeficient athymic mice, respectively, as described in the Materials and Methods. The resulting tumors were subsequently allowed to reach a mean tumor volume of 100 mm^3 before CFI-402257 drug administration began. For these experiments, CFI-402257 was administered at different doses (6.5 or 8.5 mg/kg for 129S2/SVPasCrl mice and independently with 5.0 or 6.5 mg/kg for athymic mice) by oral gavage once daily for 3 weeks.

As in Fig. 4A, when 393P murine syngeneic mice were treated with CFI-402257 for 3 weeks, the RTVs of vehicle versus 6.5- or 8.5-mg/kg–treated groups were 11.3, 5.1, and 2.7, respectively. Thus, CFI-402257 treatment statistically significantly inhibited lung cancer growth *in vivo* (6.5 mg/kg group vs. vehicle group: $P < 0.001$; 8.5 mg/kg group vs. vehicle group: $P < 0.001$). There was no appreciable treatment-induced body weight loss or observed toxicities or death that followed CFI-402257 treatments during the study period. Thus, CFI-402257 treatment was well tolerated in mice at dosages that exerted statistically significant antitumorigenic effects, as in Fig. 4B. Excised tumors were weighed after completion of CFI-402257 or vehicle treatments and inhibition rates of treated groups were calculated according to average tumor weights. The inhibition rates of the 6.5 mg/kg and 8.5 mg/kg treatment groups were 44.9% and 75.2%, respectively, as displayed in Fig. 4C; Supplementary Fig. S4A. Similar results were observed after treatment of athymic mice bearing H1299 xenografts. Examined CFI-402257 treatment dosages (5.0 and 6.5 mg/kg) statistically significantly repressed lung cancer growth (for the 5.0 mg/kg group vs. vehicle control group, $P < 0.05$, and for the 6.5 mg/kg group vs. vehicle was $P < 0.01$) without observed toxicities (see Fig. 4D–F; Supplementary Fig. S4B).

Pathways that cooperate with TTK inhibition

To uncover downstream pathways regulated by TTK inhibition that potentially cooperate with CFI-402257 treatment and augment repression of lung cancer growth, an RPPA-based investigation was undertaken. Lung tumors were harvested after independent vehicle or 6.5 mg/kg or 8.5 mg/kg CFI-402257 5-day treatments. Expression profiles of 304 critical growth-regulatory proteins were studied by RPPA and results are shown in Fig. 4G; Supplementary Fig. S4C. Profiles of expressed proteins that were consistently associated with induced growth inhibition and apoptosis of the indicated lung cancers included mTOR and Bcl-xL that were each statistically significantly altered across these different CFI-402257 treatment dosages. These results linked changes in protein expression to antineoplastic effects after TTK inhibition.

It was next sought to learn whether a correlation existed between TTK mRNA expression using TCGA database and growth-regulatory protein profiles displayed in the RPPA database. Figure 5A shows those species that were significantly correlated with TTK expression in TCGA database. Intriguingly, key components of the MAPK signaling pathway were highlighted including MEK1, p44/42 MAPK (Erk1/2), and c-Raf proteins. Expression of these species was consistently affected by CFI-402257 treatment across at least one of the examined treatment doses. Phosphorylation species of these proteins were augmented after these CFI-402257 treatments. This raised the prospect that CFI-402257 treatment was directly linked to the observed increase in MAPK activity. This hypothesis was supported by immunoblot analyses of lung cancer cells. Phosphorylation of MEK and ERK proteins each increased in examined murine (393P) and human (A549) lung cancer cells that were independently treated with 40, 200, or 1,000 nmol/L dosages of CFI-402257, but their total protein expression levels were not appreciably affected (Fig. 5B).

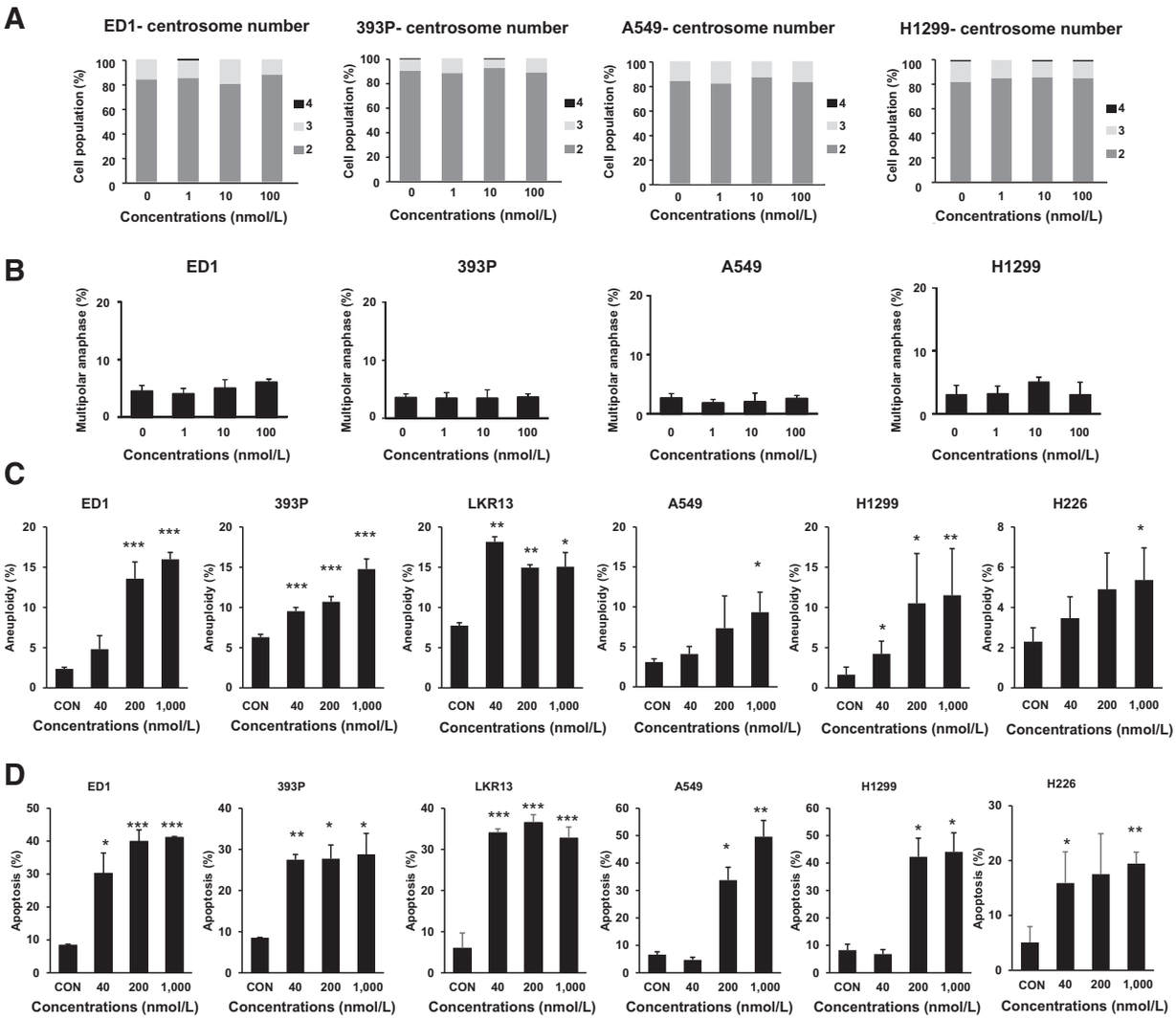

Figure 3.

CFI-402257 treatment did not appreciably change centrosome number or multipolar anaphase. **A,** Percentages of cells with different centrosome numbers after CFI-402257 treatment for 24 hours in murine (ED1 and 393P) and human (A549 and H1299) lung cancer cells. **B,** Percentages of cells undergoing multipolar anaphase after CFI-402257 treatment for 24 hours in murine (ED1 and 393P) and human (A549 and H1299) lung cancer cells. Polyploidy and apoptosis were each augmented by CFI-402257 treatment. **C,** Individual cells were treated with CFI-402257 at indicated concentrations for 48 hours before cells were harvested and fixed. The examined lung cancer cells were then stained with PI and analyzed by flow cytometry. DNA polyploidy was confirmed as the presence of peaks outside the diploid to tetraploid range. **D,** The percentages of apoptotic cells after CFI-402257 treatment for 72 hours for murine (ED1, 393P, and LKR13) and human (A549, H1299, and H226) lung cancer cells. *, $P < 0.05$; **, $P < 0.01$; ***, $P < 0.001$.

The MAPK pathway acts as an oncogenic signal to promote cancer cell survival, proliferation, metastasis, and drug resistance (44, 45). Increased activity of MAPK pathway was hypothesized to interfere with the observed antineoplastic effects of CFI-402257 treatment. Whether combining inhibitors that targeted MAPK pathway components with the TTK antagonist CFI-402257 affected antineoplastic response was explored. As shown in Fig. 5C; Supplementary Fig. S5B, the ERK1/2-specific inhibitor SCH772984 and CFI-4020257 had synergism at relatively low concentrations, using the Chou and Talalay assay, as described previously (46). Independent analysis of the relationship between clinical survival in lung cancer and expression of MAPK or TTK expression was conducted using TCGA. Notably, MAP2K1 (MEK1)- or MAP2K2 (MEK2)-high expression when combined with TTK-high expression profiles in lung adenocarcinomas indicated an unfavorable survival (Fig. 5D; Supplementary Fig. S5A). Together, these analyses provide a strong rationale for combining a MAPK pathway inhibitor with a TTK inhibitor to combat lung cancer.

Discussion

SAC functions to prevent chromosome missegregation, ensuring precise cellular division and cell proliferation (47). Targeting this process is an appealing antineoplastic strategy (2, 4–6). SAC function depends on TTK activity, which makes it a promising

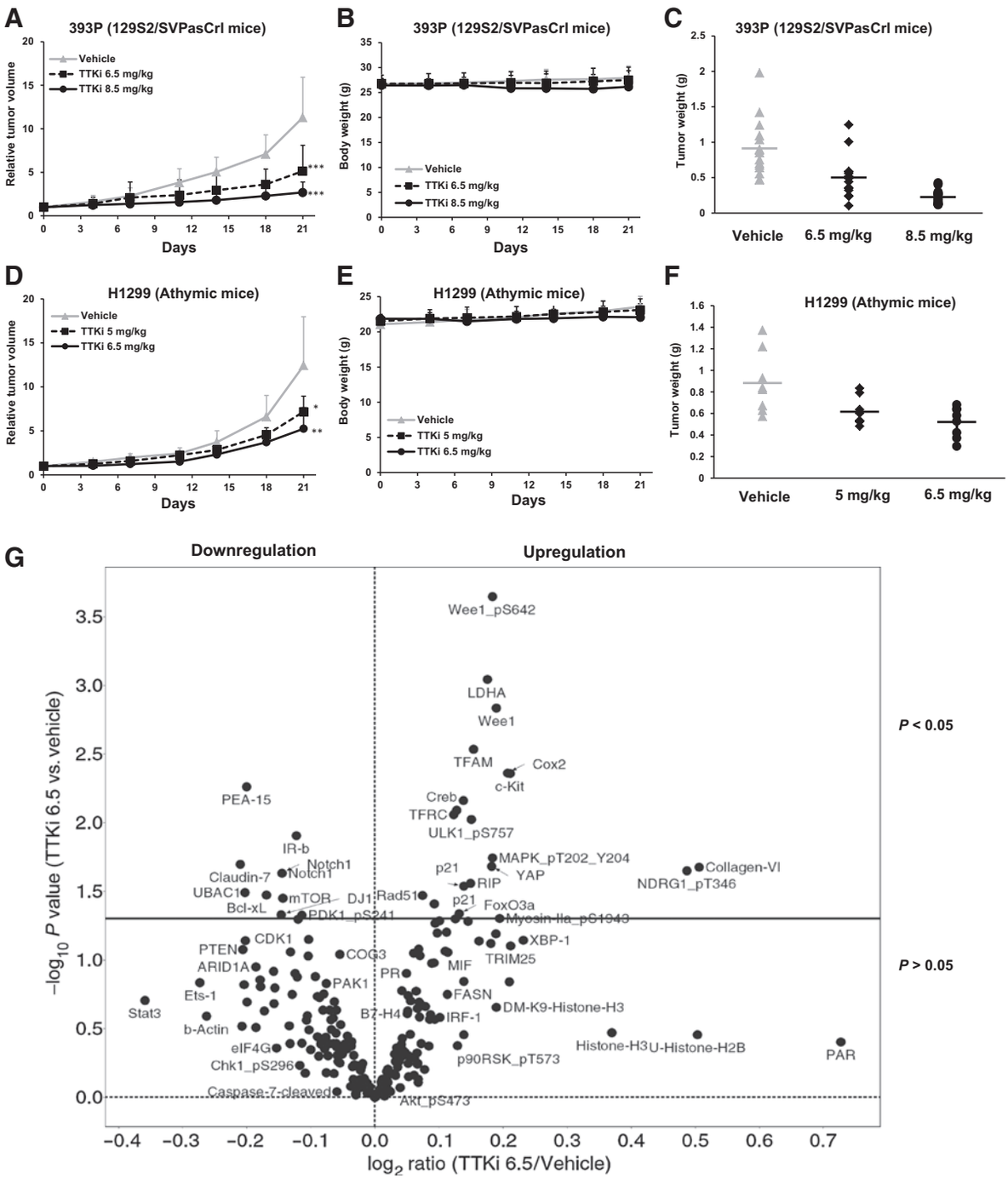

Figure 4.

In vivo antitumorigenic effects of CFI-402257 treatment. **A,** The 393P lung cancer cell line growth in 129S2/SVPasCrl mice was examined after treatment with vehicle, 6.5 mg/kg, or 8.5 mg/kg of CFI-402257. Day 0 is the treatment start date. The RTVs are expressed as the mean ± SD ($n = 15$ mice per group). **B,** Body weights of mice did not significantly change during these treatments. The average body weight of each group is shown as mean ± SD ($n = 15$ mice per group). **C,** Comparisons of excised tumor weights after these treatments. Each symbol represents the tumor weight of a single mouse. **D,** Comparison of H1299 lung cancer cell line growth in athymic mice treated with vehicle, 5.0 mg/kg, or 6.5 mg/kg of CFI-402257 treatment. Day 0 is the treatment start date. The RTVs were expressed as the mean ± SD ($n = 8$ mice per group). **E,** The average body weight of each group is shown as mean ± SD ($n = 8$ mice per group). **F,** Comparisons of excised tumor weights after these treatments are shown. Each symbol represents the tumor weight from a single mouse. **G,** Protein expression was analyzed using RPPA of cell lysates from syngeneic 393P lung cancer cell line–derived tumors treated with vehicle or with CFI-402257 for 5 days. The 393P tumor-bearing mice were treated with vehicle or 6.5 mg/kg CFI-402257 orally for 5 days, after which tumors were harvested for RPPA analyses ($n = 5$ mice per group). When comparing 6.5 mg/kg CFI-402257 with vehicle-treated controls, the proteins above the solid black line are significantly different ($P < 0.05$).

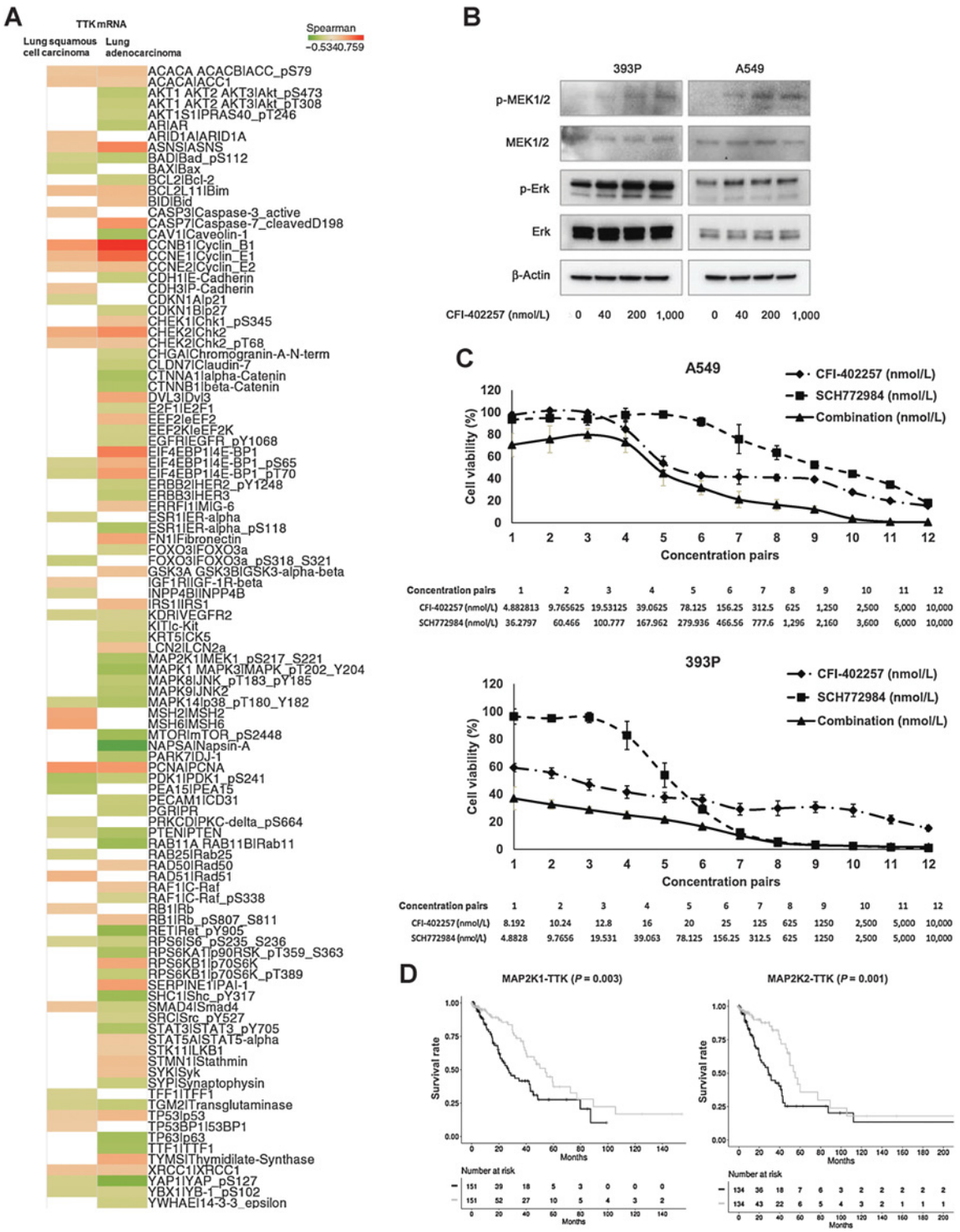

Figure 5.

Interactions between TTK inhibition and the MAPK pathway. **A,** RPPA species that significantly correlated with TTK mRNA expression are displayed from TCGA (green, negative correlation with TTK; red, positive correlation with TTK; $n = 181$ for adenocarcinomas; $n = 192$ for SCCs). **B,** CFI-402257 treatment increased activity of the MAPK pathway. Cells were independently treated with 40, 200, or 1,000 nmol/L of CFI-402257 for 72 hours, when protein extracts were immunoblotted with desired antibodies. **C,** The antiproliferative effects of CFI-402257 alone or in combination with the MAPK inhibitor SCH772984 are displayed at 72 hours. **D,** The association is shown between survival, and expression of MAP2K1/MAP2K2 and TTK species (gray, MAP2K low/TTK low; black, MAP2K high/TTK high).

anticancer therapy (48). This study explored the relationship between TTK expression and lung cancer biology. TTK expression was statistically significantly, higher in lung cancers than in corresponding normal lung tissues, while TTK mutations were rare in lung cancers (Supplementary Fig. S6). This conferred an unfavorable survival in these lung cancer cases. This insight into lung cancer biology was built upon by determining whether the TTK inhibitor, CFI-402257, is active against lung cancers *in vitro* or *in vivo*.

The TTK inhibitor, CFI-402257, exhibited potent antineoplastic activity against both murine and human lung cancers. No single-gene mutation was reported to drive either the response or resistance to TTK inhibition in the examined cancer cells (14). Consistent with this prior work, lung cancer cells were highly responsive to CFI-402257 treatment, independent of expression of the *KRAS* oncoprotein, which would address an unmet therapeutic need in oncology, as reviewed (33). Likewise, expression of the mutant p53 protein alone or with the *KRAS* oncoprotein did not appear to affect TTK inhibitor response.

Aneuploidy or chromosomal instability (CIN) occurs in most human solid tumors (49). Their roles in cancer biology are complex. It is an unresolved question whether they act as a consequence or driver of tumorigenesis or as an antineoplastic target (22). These processes lead to changes in mRNA and protein expression of growth-regulatory genes including oncogenes and tumor suppressors (33, 49). The balance between these tumorigenic and antitumorigenic effects of aneuploidy or CIN determines whether cancer growth is enhanced or repressed (22). Aneuploidy and CIN can lead cancer cells to have phenotypic variation and heterogeneity. This allows cancers to survive, progress, or respond to or become refractory to antineoplastic treatments (50). Aneuploidy and CIN can trigger lethal DNA damage and genomic instability (51). This study of the TTK inhibitor, CFI-402257, for treatment of lung cancers revealed an increase in polyploid cancer cells occurs after this drug treatment. This increase in CIN likely reached a critical threshold that caused death of the treated cancer cells.

Drug combinations could augment therapeutic activity of a TTK inhibitor. This might even overcome resistance to a TTK antagonist. Given this, an approach was taken to uncover potential antineoplastic pathways that cooperate with TTK antagonism. Bioinformatic examination of RPPAs performed in CFI-402257–treated syngeneic murine lung cancers, coupled with interrogation of TCGA databases, identified candidate cooperating targets (see Fig. 5). Antineoplastic effects of CFI-402257 treatment were associated with an increase in expression of the key growth regulator, MAPK. When coupled with treatment with a TTK inhibitor, MAPK antagonism augmented TTK antineoplastic effects. Prior work found that MAPK activity increased TTK phosphorylation at the M-phase of the cell cycle, but how TTK activity precisely affects MAPK signaling remains to be discerned (52). This is the subject of future work because cooperative antineoplastic effects were observed between TTK antagonism and MAPK inhibition, as shown in Fig. 5.

The MAPK pathway is deregulated in diverse human cancers (44). MAPK signaling occurs through a cascade of steps that act downstream of cell surface receptors, including the EGFR and the RAS oncoprotein (53). Activated ERKs phosphorylate substrates including growth-regulatory transcription factors (44). The MEK-ERK cascade affects cancer cell proliferation, survival, and metastasis, underscoring the broad functional role played by this pathway in human cancer biology (53). Independent analyses of TCGA and RPPA databases found that augmented expression of MAPK pathway components (MAP2K1 and MAP2K2) and TTK were linked to the biology of lung cancers. It was therefore not surprising that an ERK inhibitor augmented the antineoplastic effects of CFI-402257. It is proposed here that pharmacologic repression of these species will augment activity of a TTK inhibitor in the cancer clinic.

In summary, the TTK inhibitor, CFI-402257, exerts marked antineoplastic effects against both murine and human lung cancers. This likely occurred by promoting lethal levels of polyploidy within these cancer cells. The mechanistic basis for cooperation between this TTK inhibitor and a MAPK antagonist should be pursued in the laboratory. The insights obtained would provide a rationale for exploring this cooperation in the lung cancer clinic.

Disclosure of Potential Conflicts of Interest

D.W. Cescon reports receiving a commercial research grant from Pfizer, other commercial research support from Merck and GSK, has ownership interest in a patent (Biomarkers of TTK inhibitors), and has consultant/advisory board relationship with Merck, Roche, Novartis, Pfizer, Puma, Dynamo Therapeutics, Agendia, and GSK. No potential conflicts of interest were disclosed by the other authors.

Authors' Contributions

Conception and design: L. Zheng, M. Kawakami, T.W. Mak, X. Liu, E. Dmitrovsky
Development of methodology: L. Zheng, M. Kawakami, W. Lu, B. Mino, J. Rodriguez-Canales, I.I. Wistuba, X. Liu, E. Dmitrovsky
Acquisition of data (provided animals, acquired and managed patients, provided facilities, etc.): L. Zheng, M. Kawakami, Y. Chen, C. Behren, B. Mino, L.M. Solis, J. Silvester, K.L. Thu, D.W. Cescon, J. Rodriguez-Canales, I.I. Wistuba
Analysis and interpretation of data (e.g., statistical analysis, biostatistics, computational analysis): L. Zheng, Z. Chen, M. Kawakami, Y. Chen, J. Roszik, L.M. Mustachio, P. Villalobos, K.L. Thu, D.W. Cescon, X. Liu, E. Dmitrovsky
Writing, review, and/or revision of the manuscript: L. Zheng, M. Kawakami, Y. Chen, J. Roszik, L.M. Solis, D.W. Cescon, I.I. Wistuba, X. Liu, E. Dmitrovsky
Administrative, technical, or material support (i.e., reporting or organizing data, constructing databases): Z. Chen, L.M. Solis, X. Liu, E. Dmitrovsky
Study supervision: Z. Chen, D.W. Cescon, X. Liu, E. Dmitrovsky
Other (provided cell lines and collaborated on experiments): J.M. Kurie

Acknowledgments

This work was supported partly by NIH, NCI grants R01-CA087546 (to E. Dmitrovsky), R01-CA190722 (to J.M. Kurie and X. Liu), NCI contract #HHSN261200800001E, a Samuel Waxman Cancer Research Foundation Award (to E. Dmitrovsky), UT-STARs award (to E. Dmitrovsky), and an American Cancer Society Clinical Research Professorship (to E. Dmitrovsky). The authors thank Jianling Zhou, Auriole Tamegnon, and Mei Jiang in the TMP-IL Laboratory at MD Anderson Cancer Center for their help with performing ISH studies. The authors thank all members of the Mak and Dmitrovsky laboratories for their helpful consultations and Dr. Adi Gazdar at the University of Texas Southwestern (Dallas, TX) for generously providing lung cancer cell lines.

The costs of publication of this article were defrayed in part by the payment of page charges. This article must therefore be hereby marked *advertisement* in accordance with 18 U.S.C. Section 1734 solely to indicate this fact.

Received August 2, 2018; revised December 18, 2018; accepted July 24, 2019; published first July 29, 2019.

References

1. Vermeulen K, Van Bockstaele DR, Berneman ZN. The cell cycle: a review of regulation, deregulation and therapeutic targets in cancer. Cell Proliferation 2003;36:131–49.
2. Gabrielli B, Brooks K, Pavey S. Defective cell cycle checkpoints as targets for anti-cancer therapies. Front Pharmacol 2012;3:9.
3. Dominguez-Brauer C, Thu KL, Mason JM, Blaser H, Bray MR, Mak TW. Targeting mitosis in cancer: emerging strategies. Mol Cell 2015;60:524–36.
4. Lara-Gonzalez P, Westhorpe FG, Taylor SS. The spindle assembly checkpoint. Curr Biol 2012;22:R966–80.
5. Kwiatkowski N, Jelluma N, Filippakopoulos P, Soundararajan M, Manak MS, Kwon M, et al. Small-molecule kinase inhibitors provide insight into Mps1 cell cycle function. Nat Chem Biol 2010;6:359–68.
6. Liu Y, Lang Y, Patel NK, Ng G, Laufer R, Li SW, et al. The discovery of orally bioavailable tyrosine threonine kinase (TTK) inhibitors: 3-(4-(heterocyclyl)phenyl)-1H-indazole-5-carboxamides as anticancer agents. J Med Chem 2015;58:3366–92.
7. Innocenti P, Woodward HL, Solanki S, Naud S, Westwood IM, Cronin N, et al. Rapid discovery of pyrido[3,4-d]pyrimidine inhibitors of monopolar spindle kinase 1 (MPS1) using a structure-based hybridization approach. J Med Chem 2016;59:3671–88.
8. Hewitt L, Tighe A, Santaguida S, White AM, Jones CD, Musacchio A, et al. Sustained Mps1 activity is required in mitosis to recruit O-Mad2 to the Mad1-C-Mad2 core complex. J Cell Biol 2010;190:25–34.
9. Colombo R, Caldarelli M, Mennecozzi M, Giorgini ML, Sola F, Cappella P, et al. Targeting the mitotic checkpoint for cancer therapy with NMS-P715, an inhibitor of MPS1 kinase. Cancer Res 2010;70:10255–64.
10. Tardif KD, Rogers A, Cassiano J, Roth BL, Cimbora DM, McKinnon R, et al. Characterization of the cellular and antitumor effects of MPI-0479605, a small-molecule inhibitor of the mitotic kinase Mps1. Mol Cancer Ther 2011;10:2267–75.
11. Lauze E, Stoelcker B, Luca FC, Weiss E, Schutz AR, Winey M. Yeast spindle pole body duplication gene MPS1 encodes an essential dual specificity protein kinase. EMBO J 1995;14:1655–63.
12. Grant GD, Brooks L III, Zhang X, Mahoney JM, Martyanov V, Wood TA, et al. Identification of cell cycle-regulated genes periodically expressed in U2OS cells and their regulation by FOXM1 and E2F transcription factors. Mol Biol Cell 2013;24:3634–50.
13. Jemaa M, Galluzzi L, Kepp O, Senovilla L, Brands M, Boemer U, et al. Characterization of novel MPS1 inhibitors with preclinical anticancer activity. Cell Death Differ 2013;20:1532–45.
14. Mason JM, Wei X, Fletcher GC, Kiarash R, Brokx R, Hodgson R, et al. Functional characterization of CFI-402257, a potent and selective Mps1/TTK kinase inhibitor, for the treatment of cancer. Proc Natl Acad Sci USA 2017;114:3127–32.
15. Hu Z, Fan C, Oh DS, Marron JS, He X, Qaqish BF, et al. The molecular portraits of breast tumors are conserved across microarray platforms. BMC Genomics 2006;7:96.
16. Liang XD, Dai YC, Li ZY, Gan MF, Zhang SR, Yin P, et al. Expression and function analysis of mitotic checkpoint genes identifies TTK as a potential therapeutic target for human hepatocellular carcinoma. PLoS One 2014;9:e97739.
17. Slee RB, Grimes BR, Bansal R, Gore J, Blackburn C, Brown L, et al. Selective inhibition of pancreatic ductal adenocarcinoma cell growth by the mitotic MPS1 kinase inhibitor NMS-P715. Mol Cancer Ther 2014;13:307–15.
18. Kilpinen S, Ojala K, Kallioniemi O. Analysis of kinase gene expression patterns across 5681 human tissue samples reveals functional genomic taxonomy of the kinome. PLoS One 2010;5:e15068.
19. Liu Y, Laufer R, Patel NK, Ng G, Sampson PB, Li SW, et al. Discovery of pyrazolo[1,5-a]pyrimidine TTK inhibitors: CFI-402257 is a potent, selective, bioavailable anticancer agent. ACS Med Chem Lett 2016;7:671–5.
20. Siegel RL, Miller KD, Jemal A. Cancer statistics, 2016. CA Cancer J Clin 2016;66:7–30.
21. Hanahan D, Weinberg RA. Hallmarks of cancer: the next generation. Cell 2011;144:646–74.
22. Giam M, Rancati G. Aneuploidy and chromosomal instability in cancer: a jackpot to chaos. Cell Div 2015;10:3.
23. Wagner GP, Kin K, Lynch VJ. Measurement of mRNA abundance using RNA-seq data: RPKM measure is inconsistent among samples. Theory Biosci 2012;131:281–5.
24. Kawakami M, Mustachio LM, Rodriguez-Canales J, Mino B, Roszik J, Tong P, et al. Next-generation CDK2/9 inhibitors and anaphase catastrophe in lung cancer. J Natl Cancer Inst 2017;109:djw297.
25. Ma Y, Fiering S, Black C, Liu X, Yuan Z, Memoli VA, et al. Transgenic cyclin E triggers dysplasia and multiple pulmonary adenocarcinomas. Proc Natl Acad Sci USA 2007;104:4089–94.
26. Freemantle SJ, Dmitrovsky E. Cyclin E transgenic mice: discovery tools for lung cancer biology, therapy, and prevention. Cancer Prev Res 2010;3:1513–8.
27. Liu X, Sempere LF, Ouyang H, Memoli VA, Andrew AS, Luo Y, et al. MicroRNA-31 functions as an oncogenic microRNA in mouse and human lung cancer cells by repressing specific tumor suppressors. J Clin Invest 2010;120:1298–309.
28. Wislez M, Fujimoto N, Izzo JG, Hanna AE, Cody DD, Langley RR, et al. High expression of ligands for chemokine receptor CXCR2 in alveolar epithelial neoplasia induced by oncogenic kras. Cancer Res 2006;66:4198–207.
29. Gibbons DL, Lin W, Creighton CJ, Rizvi ZH, Gregory PA, Goodall GJ, et al. Contextual extracellular cues promote tumor cell EMT and metastasis by regulating miR-200 family expression. Genes Develop 2009;23:2140–51.
30. Zheng L, Fu Y, Zhuang L, Gai R, Ma J, Lou J, et al. Simultaneous NF-kappaB inhibition and E-cadherin upregulation mediate mutually synergistic anticancer activity of celastrol and SAHA in vitro and in vivo. Int J Cancer 2014;135:1721–32.
31. Kawakami M, Mustachio LM, Zheng L, Chen Y, Rodriguez-Canales J, Mino B, et al. Polo-like kinase 4 inhibition produces polyploidy and apoptotic death of lung cancers. Proc Natl Acad Sci USA 2018;115:1913–8.
32. Gianni M, Qin Y, Wenes G, Bandstra B, Conley AP, Subbiah V, et al. High-throughput architecture for discovering combination cancer therapeutics. J Clin Oncol Clin Cancer Inform 2018;2:1–12.
33. Kawakami M, Mustachio LM, Liu X, Dmitrovsky E. Engaging anaphase catastrophe mechanisms to eradicate aneuploid cancers. Mol Cancer Ther 2018;17:724–31.
34. Chan JY. A clinical overview of centrosome amplification in human cancers. Int J Biol Sci 2011;7:1122–44.
35. Basto R, Brunk K, Vinadogrova T, Peel N, Franz A, Khodjakov A, et al. Centrosome amplification can initiate tumorigenesis in flies. Cell 2008;133:1032–42.
36. Kwon M, Godinho SA, Chandhok NS, Ganem NJ, Azioune A, Thery M, et al. Mechanisms to suppress multipolar divisions in cancer cells with extra centrosomes. Genes Develop 2008;22:2189–203.
37. Fisk HA, Mattison CP, Winey M. Human Mps1 protein kinase is required for centrosome duplication and normal mitotic progression. Proc Natl Acad Sci USA 2003;100:14875–80.
38. Kasbek C, Yang CH, Yusof AM, Chapman HM, Winey M, Fisk HA. Preventing the degradation of mps1 at centrosomes is sufficient to cause centrosome reduplication in human cells. Mol Biol Cell 2007;18:4457–69.
39. Stucke VM, Baumann C, Nigg EA. Kinetochore localization and microtubule interaction of the human spindle checkpoint kinase Mps1. Chromosoma 2004;113:1–15.
40. Stucke VM, Sillje HHW, Arnaud L, Nigg EA. Human Mps1 kinase is required for the spindle assembly checkpoint but not for centrosome duplication. EMBO J 2002;21:1723–32.
41. Hewitt L, Tighe A, Santaguida S, White AM, Jones CD, Musacchio A, et al. Sustained Mps1 activity is required in mitosis to recruit O-Mad2 to the Mad1-C-Mad2 core complex. J Cell Biol 2010;190:25–34.
42. Jemaa M, Galluzzi L, Kepp O, Senovilla L, Brands M, Boemer U, et al. Characterization of novel MPS1 inhibitors with preclinical anticancer activity. Cell Death Differ 2013;20:1532–45.
43. Szymiczek A, Carbone M, Pastorino S, Napolitano A, Tanji M, Minaai M, et al. Inhibition of the spindle assembly checkpoint kinase Mps-1 as a novel therapeutic strategy in malignant mesothelioma. Oncogene 2017;36:6501–7.
44. Dhillon AS, Hagan S, Rath O, Kolch W. MAP kinase signalling pathways in cancer. Oncogene 2007;26:3279–90.
45. Kraunz KS, Nelson HH, Liu M, Wiencke JK, Kelsey KT. Interaction between the bone morphogenetic proteins and Ras/MAP-kinase signalling pathways in lung cancer. Br J Cancer 2005;93:949–52.
46. Chou TC. Drug combination studies and their synergy quantification using the Chou-Talalay method. Cancer Res 2010;70:440–6.

47. London N, Biggins S. Signalling dynamics in the spindle checkpoint response. Nat Rev Mol Cell Biol 2014;15:736–47.
48. Abrieu A, Magnaghi-Jaulin L, Kahana JA, Peter M, Castro A, Vigneron S, et al. Mps1 is a kinetochore-associated kinase essential for the vertebrate mitotic checkpoint. Cell 2001;106:83–93.
49. Kalyana-Sundaram S, Shankar S, Deroo S, Iyer MK, Palanisamy N, Chinnaiyan AM, et al. Gene fusions associated with recurrent amplicons represent a class of passenger aberrations in breast cancer. Neoplasia 2012;14:702–8.
50. Roschke AV, Rozenblum E. Multi-layered cancer chromosomal instability phenotype. Front Oncol 2013;3:302.
51. Bakhoum SF, Kabeche L, Murnane JP, Zaki BI, Compton DA. DNA-damage response during mitosis induces whole-chromosome missegregation. Cancer Discov 2014;4:1281–9.
52. Douetts-Peres JC, Cruz MA, Reis RS, Heringer AS, de Oliveira EA, Elbl PM, et al. Mps1 (monopolar Spindle 1) protein inhibition affects cellular growth and pro-embryogenic masses morphology in embryogenic cultures of araucaria angustifolia (araucariaceae). PLoS One 2016;11:e0153528.
53. Roberts PJ, Der CJ. Targeting the Raf-MEK-ERK mitogen-activated protein kinase cascade for the treatment of cancer. Oncogene 2007;26:3291–310.